Engineering Geology 259 (2019) 105139

Contents lists available at ScienceDirect

Engineering Geology

journal homepage: www.elsevier.com/locate/enggeo

Long-term hydrogeophysical monitoring of the internal conditions of river levees

Greta Tresoldi[a,*], Diego Arosio[b], Azadeh Hojat[c,a], Laura Longoni[a], Monica Papini[a], Luigi Zanzi[a]

[a] Dipartimento di Ingegneria Civile e Ambientale, Politecnico di Milano, Milan 20133, Italy
[b] Dipartimento di Scienze Chimiche e Geologiche, Università di Modena e Reggio Emilia, Modena 41125, Italy
[c] Department of Mining Engineering, Shahid Bahonar University of Kerman, Kerman 76188, Iran

ARTICLE INFO

Keywords:
Geoelectrical methods
ERT
Embankment
Irrigation canal
Levee
Water saturation

ABSTRACT

To evaluate the vulnerability of the earthen levee of an irrigation canal in San Giacomo delle Segnate, Italy, a customized electrical resistivity tomography (ERT) monitoring system was installed in September 2015 and has been continuously operating since then. Thanks to a meteorological station deployed at the study site, we could investigate the relationship between the inverted resistivity values and different parameters, namely air temperature, rainfall and water level in the canal. Air temperature seems to have a minor but not negligible influence on resistivity variations, especially at shallow depth. A model of soil temperature versus depth was used to correct resistivity sections for air temperature variations through the different seasons. Changes of the water level in the canal and rainfall significantly affect measured resistivity values. At the study site, the most important variations of resistivity are related to saturation and dewatering processes in the irrigation periods. Although we explored the effect of drawdown procedures on resistivity data, this process, causing rapid variations of resistivity values, is still not completely understood because the canal is rapidly emptied during rainfall events. Therefore, the effect of variations of the water level in the canal on levee resistivity cannot be distinguished from the effect of rainfalls. To study the effect of water level variations alone, we considered the beginning of the irrigation period when the dry canal is gradually filled and we observed a smooth trend of resistivity changes. The effect of rainfall on the data was studied during different periods of the year and at different depths of the levee so that the resistivity variations could be evaluated under different conditions. To convert the inverted resistivity sections into water content maps, an empirical and site-dependent relationship between resistivity and water content was obtained using core samples. Water content data can then be used for the implementation of stability analysis using custom modeling. This study introduces an efficient technique to monitor earthen levees and to control the evolution of seepage and water saturation in pseudo-real time. Such a technique can be exploited by Public Administrations to reduce hydrogeological risks significantly.

1. Introduction

In the last decades, hydrogeological risks associated to levee breaches have become an important subject of study in several European countries. Nowadays, there is an increasing interest to introduce techniques that can efficiently monitor the internal conditions of embankments in order to develop early warning alarm systems. Geophysical methods have been increasingly applied to hydrogeological risk mitigation investigations to evaluate the stability conditions of dams, embankments and slopes (Fauchard and Mériaux, 2007; Inazaki, 2007; Kim et al., 2007; Asch et al., 2008; Biavati et al., 2008; Cardarelli et al., 2010; Di Prinzio et al., 2010; Hibert et al., 2012; Niederleithinger et al., 2012; Morelli and Francese, 2013; Chlaib et al., 2014; Francese and Monteiro Santos, 2014; Busato et al., 2016; Bakula et al., 2017; Borgatti et al., 2017; Crawford and Bryson, 2018). Among the different geophysical techniques, geo-electrical methods are suitable for hydrogeological studies, thanks to the fact that geo-electrical measurements can investigate variations of soil composition and water saturation, detect development of weak zones and evaluate the slope stability. In the scientific literature, electrical resistivity tomography (ERT) has been used to detect seepages through embankments, to monitor water saturation inside landslide bodies, and to identify sliding surfaces (Panthulu et al., 2001; Lapenna et al., 2005; Cho and Yeom, 2007; Chambers et al., 2008; Piegari et al., 2008; Al-Fares, 2014; Cardarelli et al., 2014; Inazaki et al., 2016; Wodajo and Hickey, 2017). Time-lapse ERT measurements have been performed mainly in structural

* Corresponding author.
E-mail address: greta.tresoldi@polimi.it (G. Tresoldi).

https://doi.org/10.1016/j.enggeo.2019.05.016
Received 13 August 2018; Received in revised form 13 April 2019; Accepted 11 May 2019
Available online 16 May 2019

assessment and stability analysis of dams, levees, and landslides (Gallipoli et al., 2000; Karastathis et al., 2002; Godio et al., 2006; Chambers et al., 2009; Kuras et al., 2009; Jomard et al., 2010; Supper et al., 2012; Takakura et al., 2013; Perri et al., 2014; Supper et al., 2014; Loperte et al., 2016; Hojat et al., 2019a). However, a very important goal would be the development of integrated autonomous systems for long-term monitoring of such structures. This objective has been partly accomplished in landslide studies and monitoring of embankments (Chambers et al., 2014: Gunn et al., 2015; Gunn et al., 2018), but there is still a considerable gap as far as monitoring of river levees is concerned.

In this research, we could benefit from the non-destructive nature of ERT to implement a systematic monitoring approach of river levees. Commercial resistivity meters are normally designed to investigate relatively deep subsurface layers and thus they inject large currents into the ground. This characteristic is beyond the needs of our application. Moreover, commercial instruments are portable and cannot be installed permanently because they lack appropriate features. Therefore, a prototype of resistivity meter was designed and permanently installed in a test site in 2015. The main objective is to evaluate changes in resistivity values in order to monitor water saturation and seepage zones in the structure. The prototype is designed with peculiar characteristics to investigate shallow depths, it is relatively low-price, it can be powered by solar panels, it operates and is programmed remotely and sends the data over the internet to a web server.

2. Materials and methods

The test site selected for permanent installation of the ERT system is the earthen levee of an irrigation canal in San Giacomo delle Segnate, Mantova, Northern Italy (Fig. 1). This site was suggested by Consorzio di Bonifica Terre dei Gonzaga in Destra Po, the managing authority responsible for maintenance of canals in the area. Although the canal was grouted, we observed several problems that could be related to seepage and internal erosions. The section of the levee selected for this study is critical because it is located in the center of the village and surrounded by large flat areas. Therefore, monitoring the levee is very important to reduce the hydrogeological risks and to plan proper maintenance activities.

After about one year of preliminary time-lapse ERT tests with a commercial resistivity meter (IRIS Syscal Pro), the customized system was permanently installed along the levee on 15 September 2015. We dug a 0.5 m-deep trench in the middle of the levee crest where we deployed two cables equipped with 48 1 m-spaced plate electrodes (Fig. 2). We decided to perform the measurements with the Wenner configuration, so the maximum investigation depth is about 7-8 m, and the vertical and horizontal resolutions are 0.5 m and 1 m, respectively. This configuration is ideal to monitor the inner situation of embankments where shallow investigations with good resolution are required. To protect the cables from rodents, we used a robust anti-rodent plastic case for the cables and the connections with the electrodes were sealed with a bi-component resin. The system is totally autonomous and can operate and be programmed remotely. It is powered by a solar panel and all the parameters of daily measurements including the injected current, measured voltage, used quadrupole, quality factor, and resistivity values are saved in a text file and sent to the research center through internet connection. The frequency of measurements can be changed remotely according to the level of risk. The maximum injected current of 200 mA is suitable for shallow investigations. When requested remotely, the system can perform a contact resistance check (Arosio et al., 2017; Tresoldi et al., 2018).

Fig. 1. Test site showing the irrigation canal and the monitored levee on the left.

Besides reducing hydrogeological risk, permanent monitoring can be very useful to understand saturation and dewatering of the levee structure, as well as to analyze how resistivity values are related to annual variations of the water content according to the irrigation season. Fig. 3 shows two examples of the pseudo-sections recorded in winter with empty canal, and in summer when the water level was maximum. The winter data show higher apparent resistivity values due to the fact that the levee was dry, while the summer data show lower apparent resistivity values because of saturation of the embankment.

The datasets recorded by the monitoring system were individually inverted with Res2DInv software using the L2-norm option. Fig. 4 shows the inverted resistivity sections for the measured pseudosections shown in Fig. 3. A deep layer of low resistivity remains approximately constant through different seasons. This low resistivity zone is attributed to a deep layer of alluvial clay. Down to 3 m depth we can observe large changes related to variations of the water level in the canal. The embankment is about 3.80 m high and thus, saturation and dewatering processes can affect the levee body. Decrease in resistivity values during the irrigation period is not homogeneous along the ERT profile and shows a central zone with very low values. We decided to focus on this section of the levee to understand how resistivity is affected by seasonal changes of water level, rainfall events and air temperature.

3. Results

3.1. Effects of external variables

Thanks to data collected by the meteorological station in the study area, we studied the effects of temperature, water level and rainfall events on resistivity for more than two years. We point out that the meteorological station and the resistivity-meter have sampling intervals of 10 minutes and 1 day, respectively. This difference may prevent the analysis of relatively fast resistivity variations caused by intense meteorological events, although resistivity changes are generally slower than climatic ones. To tackle this drawback, the prototype sampling frequency can be modified remotely, though energy consumption issues should be considered. In order to better compare meteorological and resistivity datasets, we computed daily averages for temperature and water level data, while rainfall was cumulated over the 24 hours prior to resistivity measurements.

3.1.1. Air temperature

Previous studies report that daily variations of air temperature may affect the resistivity measurements down to 1 m depth only (Samoüelian et al., 2005; Afa and Anaele, 2010; Brunet et al., 2010). However, long-term seasonal cycles of air temperature can affect soil temperature down to > 5 m (Hayley et al., 2007; Hayley et al., 2010; Chambers et al., 2014). Therefore, we studied the resistivity changes due to temperature variations at different depths in terms of both air and soil temperatures.

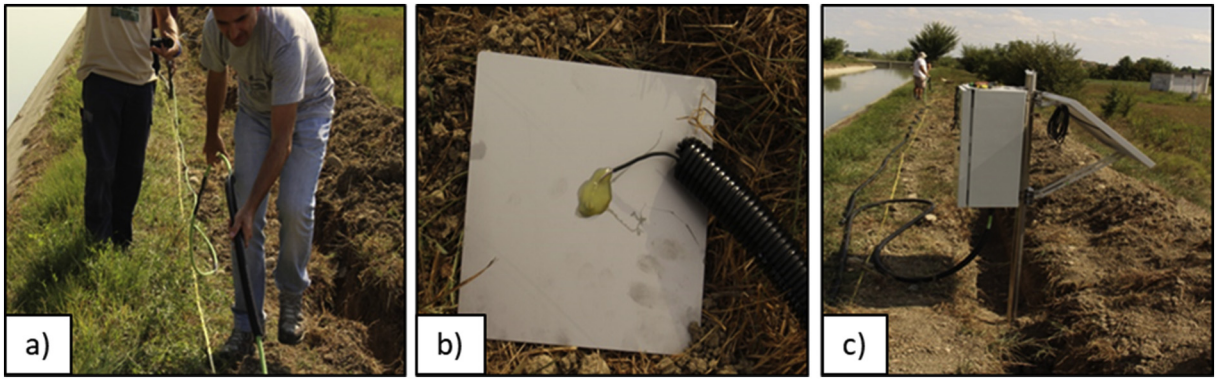

Fig. 2. Installation of the prototype system on 15 September 2015. a) Cables were covered with anti-rodent plastic case. b) Plate electrode. c) Deployment of the box containing the resistivity-meter.

At first, we produced scatter plots of air temperature, soil temperature, and inverted resistivity values at different times of the year. We used soil temperature data measured in 2016–2017 with a TDR probe placed at 1 m depth. In order to separate the influence of rainfall, which plays an important role on resistivity distribution (see following paragraph), we selected just one measurement per week, possibly far from any rainfall event.

For the resistivity values, we computed the mean values of the inverted sections at 0.50 m, 1.55 m, and 2.80 m depth, i.e. at the surface, at the intermediate depth and at the bottom of the levee. The comparison that follows, where soil temperature was measured at 1m depth only, is a qualitative analysis aimed at evaluating the necessity of temperature corrections. For quantitative temperature corrections, soil temperature was modelled at different depths with an empirical mathematical relation that will be discussed later.

Fig. 5 shows different trends of resistivity versus soil temperature in 2017. Shallow resistivity is expected to be inversely related to temperature, but for our data the role of temperature is overridden by other factors, such as drying of the top of the embankment in summer and wetting in winter because of longer rainfall periods. At intermediate depth, the resistivity trend is consistent with temperature: as the temperature increases, resistivity decreases. However, we should also consider the role of water level in the canal, which is higher during the irrigation season (i.e., spring and summer). Thus, the two effects cannot be distinguished on this plot. The bottom part of the levee has a gentle decreasing trend due to both increasing soil temperature and water in the canal.

In order to separate the effects of water level in the canal and temperature, we considered a time span with few rainfalls, no water in the canal and large temperature variations. In more detail, we selected January 2016 because the temperature changed from $> 15\,^{\circ}C$ to $-5\,^{\circ}C$ in a few days and few precipitations occurred. In Fig. 6 we show air and soil temperatures at the time of each ERT measurement (5 p.m.) and inverted resistivity values averaged at 0.50 m, 1.55 m and 2.80 m depth. Measured air temperature values are delayed of about three days in order to simulate the heat diffusion process within the soil.

According to Fig. 6, the resistivity of the shallow layer increases about 2Ωm as the air temperature decreases abruptly and decreases the same amount when air temperature begins to increase. The resistivity at intermediate depth (approximately the depth of the TDR probe) increases 1.8Ωm following $1.9\,^{\circ}C$ decrease of soil temperature. The resistivity of the bottom part of the levee does not change with temperature.

Scatter plots of the mean resistivity versus air and soil temperatures in January 2016 were also created to analyze more carefully the role of temperature during winter. Fig. 7shows that the electrical behavior of the levee at shallow depth is influenced by the variations of air temperature with a time-lag of about three days. The plot confirms the inverse proportionality between shallow resistivity and air temperature, as illustrated also in Fig. 6.

Similarly, the scatter plot in Fig. 8 confirms the inverse proportionality between resistivity at the intermediate depth and soil temperature.

The analysis of data collected in January 2016 allowed to isolate short-term temperature effects from the effects of rainfall and water level in the canal. On the contrary, long-term temperature effects can be masked by other major effects with either constructive or descructive interference. Nevertheless, temperature modifies the soil electrical response to variations of other parameters.

To predict and compensate the influence of periodic changes of soil

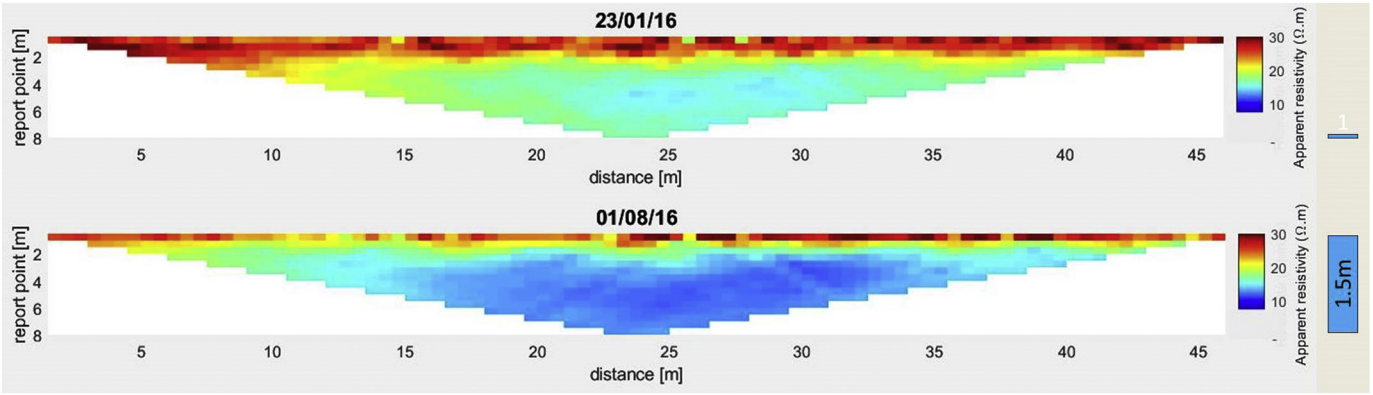

Fig. 3. Examples of apparent resistivity pseudosections obtained with the customized monitoring system in winter, 23 January 2016, (top) and summer, 1 August 2016, (bottom). The light blue bar on the right hand side indicates the water level in the canal at the time of each measurement. (For interpretation of the references to colour in this figure legend, the reader is referred to the web version of this article.)

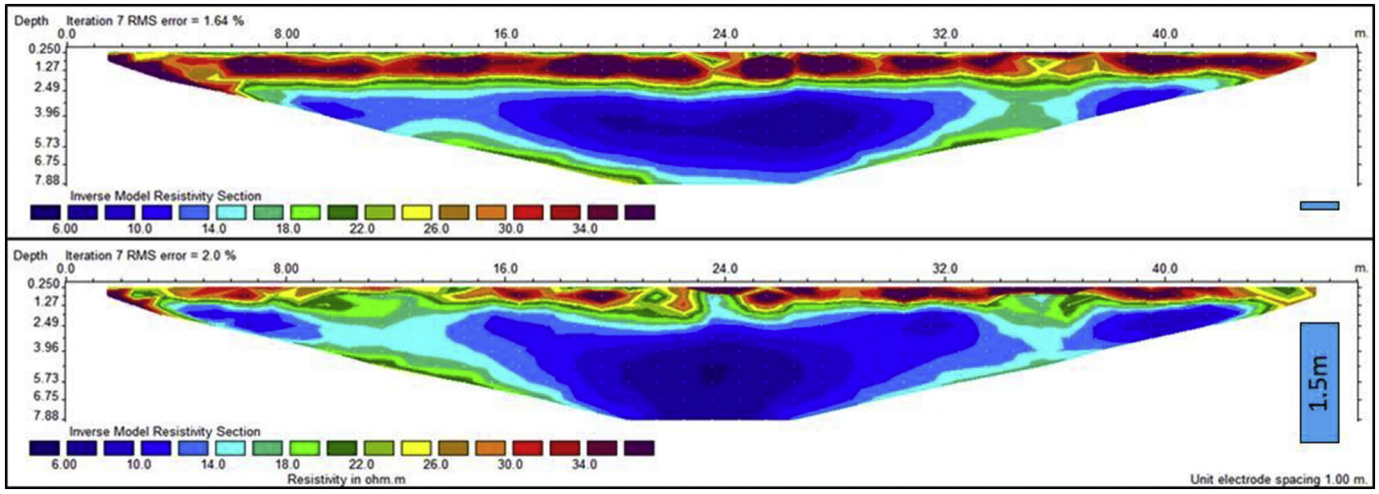

Fig. 4. Resistivity maps obtained by inverting pseudo-sections in Fig. 3. Top: 23 January 2016; bottom: 1 August 2016. The light blue bar on the right hand side indicates the water level in the canal at the time of each measurement. (For interpretation of the references to colour in this figure legend, the reader is referred to the web version of this article.)

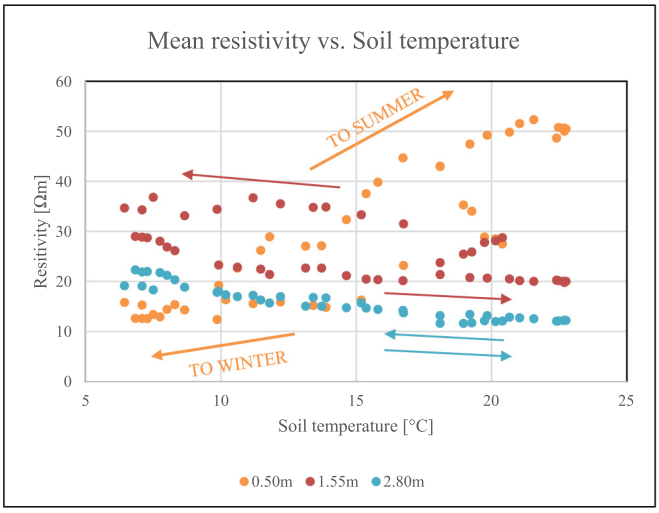

Fig. 5. Scatter plot of resistivity averaged at different depths and soil temperature at 1 m depth. The arrows indicate the passing of seasons in 2017. Arrows pointing to the right (increasing temperature) are towards summer, while arrows pointing to the left (decreasing temperature) are towards winter.

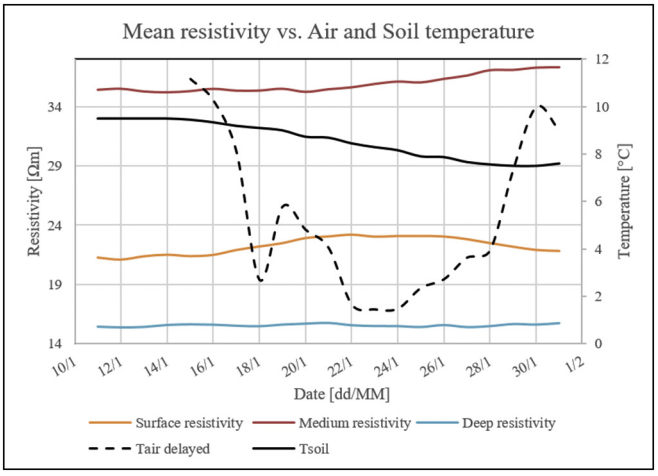

Fig. 6. The effect of air and soil temperature variations on resistivity at different depths (11–31 January 2016). The resistivity values are averaged at depths of 0.50 m, 1.55 m and 2.80 m.

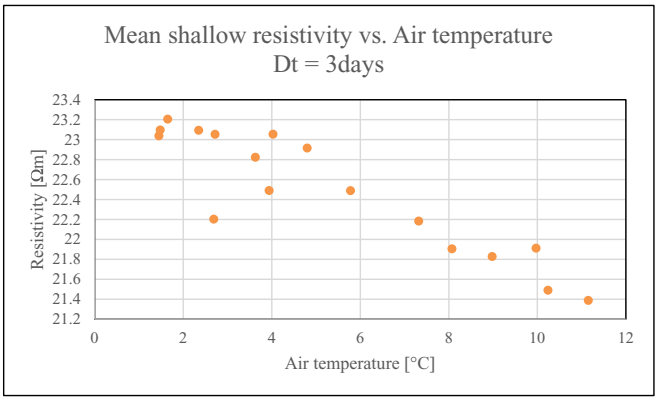

Fig. 7. Scatter plot of averaged shallow (0.50 m) resistivity and 3-day delayed air temperature from 11 to 31 January 2016.

temperature on resistivity, temperature variations down to > 5 m could be important and thus, long-term measurements of this variable at depth are required (Chambers et al., 2014). Since we sampled soil temperature just at 1 m depth, we decided to model temperature variations at different depths. We tested different relationships (Musy and Soutter, 1991; Brunet et al., 2010; Chambers et al., 2014) and we compared the modelled soil temperatures at 1 m depth with the measured values in 2016 and 2017. We found that the best-fit model is the equation proposed by Chambers et al. (2014):

$$T(z,t) = Tmean(air) + Ae^{-(z/d)}\sin\left(\omega t + \Phi - {}^{z}/_{d}\right) \quad (1)$$

where T(z,t) is the soil temperature as a function of depth and of the day of the year (from 1 to 365), T_{mean}(air) is the daily mean of air temperature, A is the maximum deviation of temperature from the mean value, d is the penetration depth, ω is the angular frequency ($2\pi/365$) and Φ is the lag of the mean value. As an example, Fig. 9 shows the modelled and measured temperatures in 2017. Throughout 2016 and 2017 we observed a maximum misfit smaller than 2°C.

After calibrating the parameters, we computed soil temperature for depths from 0.5 m to 7.5 m (penetration depth of ERT measurements) for 2016 and 2017. Fig. 10 illustrates the curves of the modelled soil temperature in 2017 down to the depth of 4 m. At greater depths, no variations during the different seasons are noticeable. It is clear that

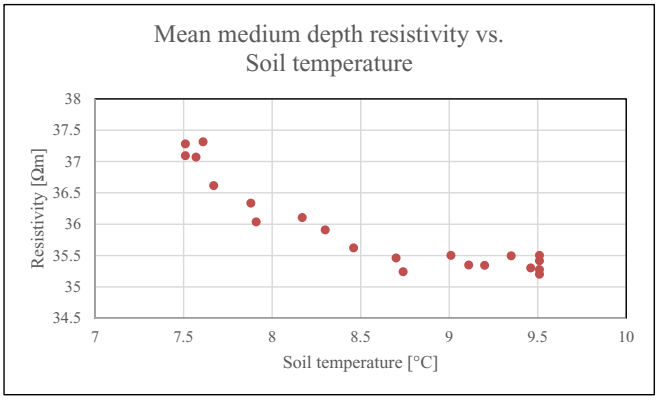

Fig. 8. Scatter plot of averaged intermediate-depth (1.55 m) resistivity and soil temperature from 11 to 31 January 2016.

changes in the soil temperature are damped and delayed with depth due to the process of heat transfer.

The soil temperature values were then used to correct resistivity data according to Eq. (2), from Hayley et al. (2007), where the resistivity measured at temperature T is modified as it was measured at T_{mean}. The coefficient α that links the variation of temperature with resistivity is 0.02 $°C^{-1}$, indicating that resistivity decreases 2% for a temperature increase of 1 °C.

$$\rho_{Tmean} = \rho_T * (1 + \alpha * (T - T_{mean})) \quad (2)$$

3.1.2. Rainfall and water level in the canal

Having corrected the data for the temperature effect, we calculated averages resistivity values for each depth level to analyze the relation between variations of resistivity at each depth and changes of other external parameters. We considered six different depths: 0.5 m and 1 m corresponding to the shallow part of the embankment; 1.55 m, 2.15 m and 2.80 m as intermediate depths of the levee; 3.50 m as the base of the structure. We already pointed out (see Fig. 4 for example) that the water level in the canal and rainfall are two of the most important factors that determine soil water content and resistivity in the embankment. Accordingly, we studied rainfall and canal water level data to characterize the soil response to different types of water seepage, namely a horizontal flow coming from the canal and a vertical one due to rainfall infiltration.

We took into account the period from 15 July to 15 October 2016, in which the canal was progressively emptied. Unfortunately, no rainfall data are available from 18 August to 12 September because the meteorological station installed in the study site was damaged by a local rainstorm on 18 August. For any analyzed day, we computed the cumulative rainfall considering 24 h prior to resistivity measurement. Specifically, for a measurement performed on the Nth day at 1p.m., the cumulative rainfall is the sum of the precipitation from the N-1thday at 1.10 p.m. until the Nth day at 1 p.m. We point out that rainfall and drawdown in the canal are to be considered dependent variables, because the managing authority of the canals usually lowers the water level during rainfall events (Fig. 11). Obviously, this makes data interpretation more difficult, also considering that the drawdown process may start from a few hours to one day after any precipitation event.

In this study, we deem our analysis of the relationship between resistivity and rainfall is only qualitative because we neglected evapotranspiration that might play an important role especially during the summer. Nevertheless, we observed a strong relation between precipitation and resistivity variations.

e observed three main behaviors in response to lowering the water level and to rainfall events. As expected, shallow resistivity measurements of the levee are strongly related to rainfall events (Fig. 11). Larger resistivity changes with rainfall can be observed at the depth of 0.50 m and resistivity variations down to 1.00 m depth are dependent upon the duration and rate of precipitations. On the contrary, superficial layers are not affected by drawdown processes because they are generally above the water level in the canal (the 1.00 m-deep layer was below the water level just for one month). These results show that the upper part of the embankment is dominated by rainfall infiltration and seepage has a strong vertical component down to 1.00 m depth. On the contrary, intermediate depths might be strongly influenced by the water level in the canal but Fig. 11 shows how rainfall and water level are closely connected: after any major precipitation event, water level in the canal is lowered. Thus, the individual effect of rainfall and water level cannot be distinguished during this season and we have to discuss the combined effect of the two variables.

At depths between 1.55 m and 2.80 m, resistivity values slowly decrease with constant water level, while they increase rapidly as a consequence of rainfall and of water level drop. To evaluate whether this last effect is physically meaningful or an artefact caused by inversion, Fig. 12 illustrates apparent resistivity values and rainfall data for the same period. The result is that measured apparent resistivity values at 1.5 m and 2.5 m pseudo-depths also increase quite fast during rainfalls, while they decrease slowly or remain approximately constant when no precipitation occurs. Compared to intermediate depths, the base of the embankment presents an opposite trend, with resistivity values reduced after rainfalls. This was observed for both inverted and apparent resistivity values (Figs. 11 and 12). This behavior can be explained by considering that there is a ditch near the base of the levee to collect water from the irrigation canal. This trench promotes collection of rainfall water and produces a horizontal seepage from the external side of the embankment.

In order to study resistivity changes due to the individual effect of

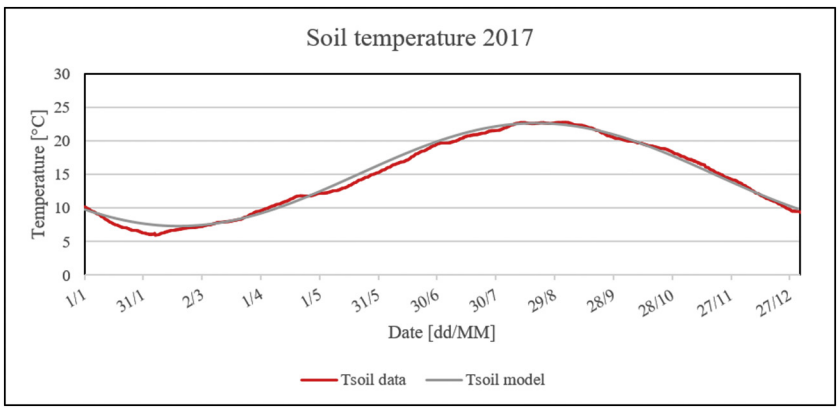

Fig. 9. Measured and modelled soil temperatures at 1 m depth in 2017.

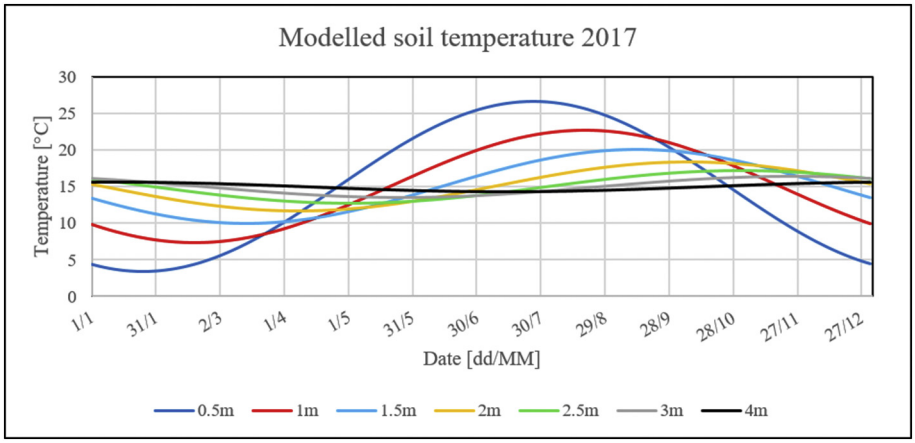

Fig. 10. Modelled soil temperature variations with depth during 2017.

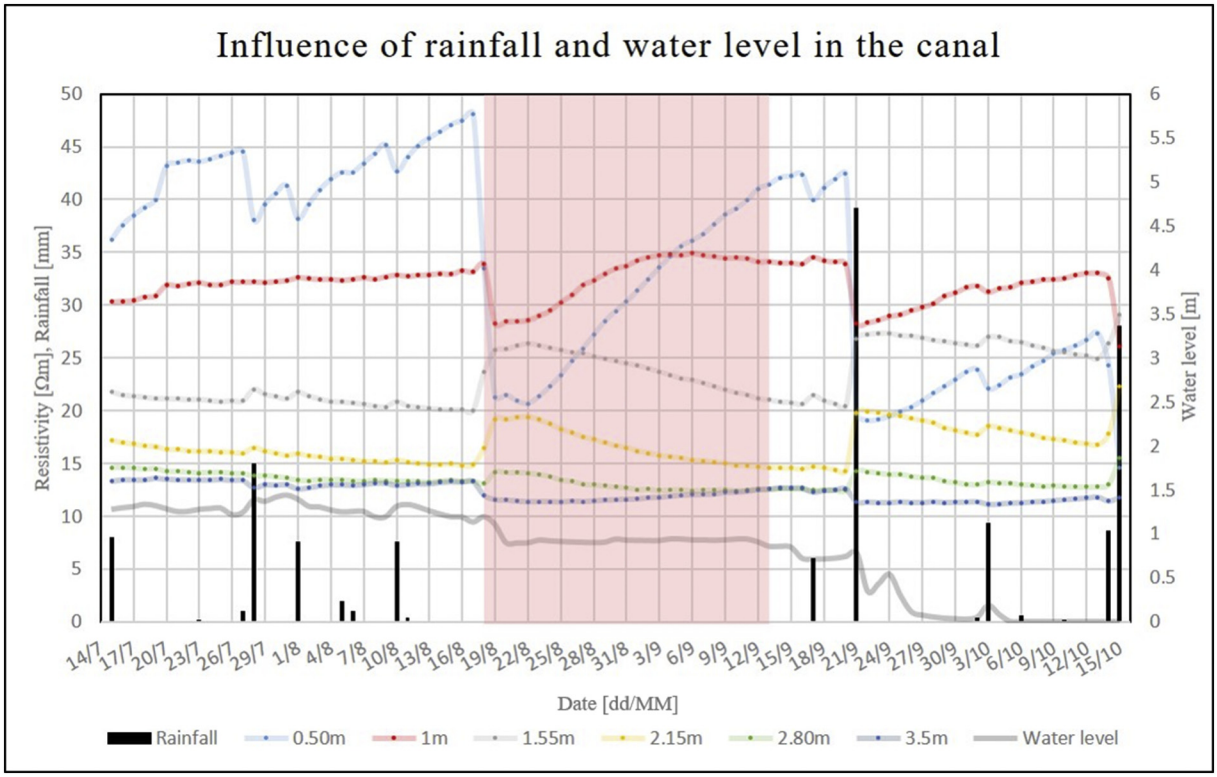

Fig. 11. Influence of the rainfall and water level in the canal on resistivity at different depths (15 July – 15 October 2016). The shaded area indicates the period when the rain gauge was damaged.

the variations of the water level in the canal, the data collected from 5 March to 25 April 2017 were also analyzed (Fig. 13). This is the period when the canal was filled and contrary to what happens when the water in the canal was discharged, we were able to find water level variations not related to rainfall events. The precipitation rate was quite low and the filling procedure was planned independently from rainfall events. Measurements at shallow depths (i.e., 0.50 m and 1.00 m) show an increasing trend of resistivity values because of the top soil getting dry. These measurements are not affected by the increased water level, that is quite small though. At intermediate depths and also deep depths although with much lower intensity, the resistivity values of the levee body present a smooth decreasing trend, because of the progressive saturation of the structure. No abrupt changes are recorded in this period.

As shown by the above discussion, drawdown and filling processes reveal different electrical behaviors. When lowering the water level, abrupt changes in soil resistivity are recorded, with sudden increase of resistivity at the intermediate depths of the levee. By comparing the data from the two selected periods, the rapid increase in resistivity values at intermediate depth is likely due to rainfalls rather than drawdown in the canal because the resistivity response to water level variations is slow and gradual (Fig. 13). The resistivity of rainwater is commonly higher than the resistivity of the pore water in the levee soil. Therefore, the sharp increase in resistivity measurements could be attributed to the infiltration of the rainwater in the saturated part of the levee, replacing the more conductive pore water. Further studies are required to validate this assumption and lab tests might help to distinguish the individual effects of water level and rainfall.

Scatter plots were also created to better analyze resistivity versus rainfalls and resistivity versus water level in the canal. We studied daily variations of resistivity and precipitation from 15 July to 15 October 2016 and we considered three different depths, representing the

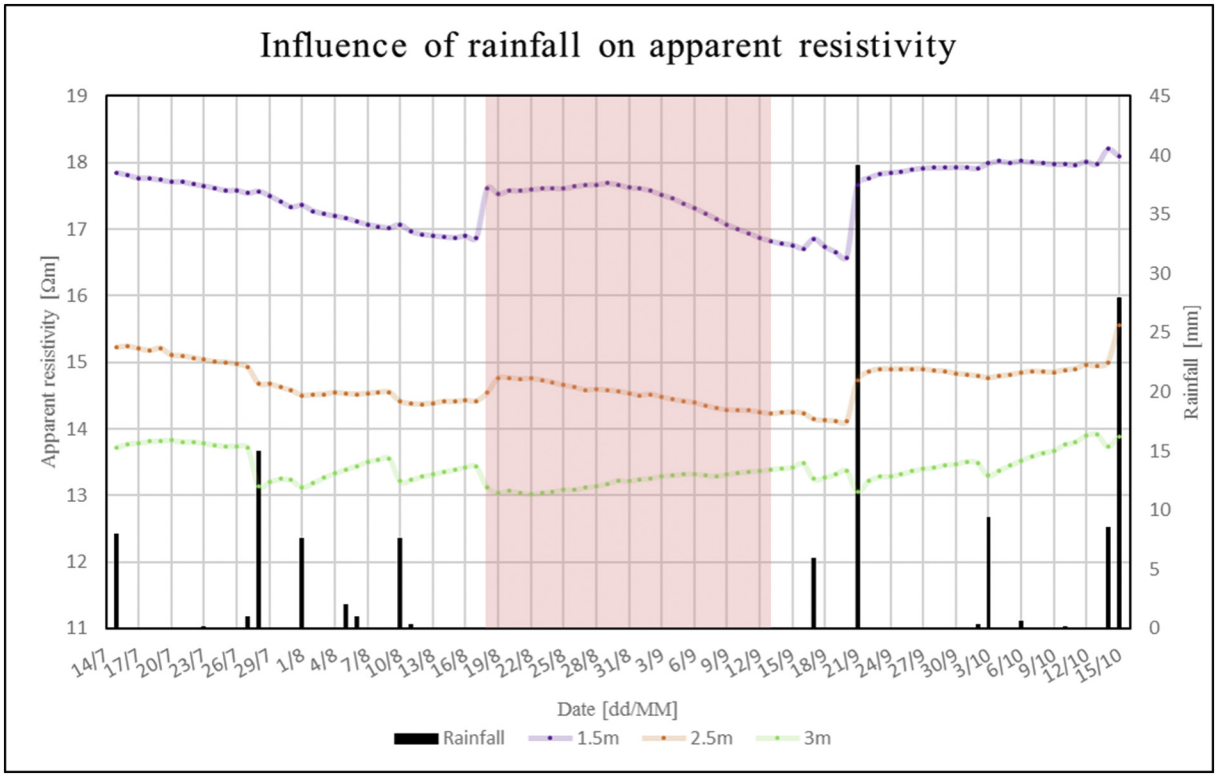

Fig. 12. Influence of rainfall on apparent resistivity values at different pseudo-depths (15 July – 15 October 2016). The shaded area indicates the period when the rain gauge was damaged.

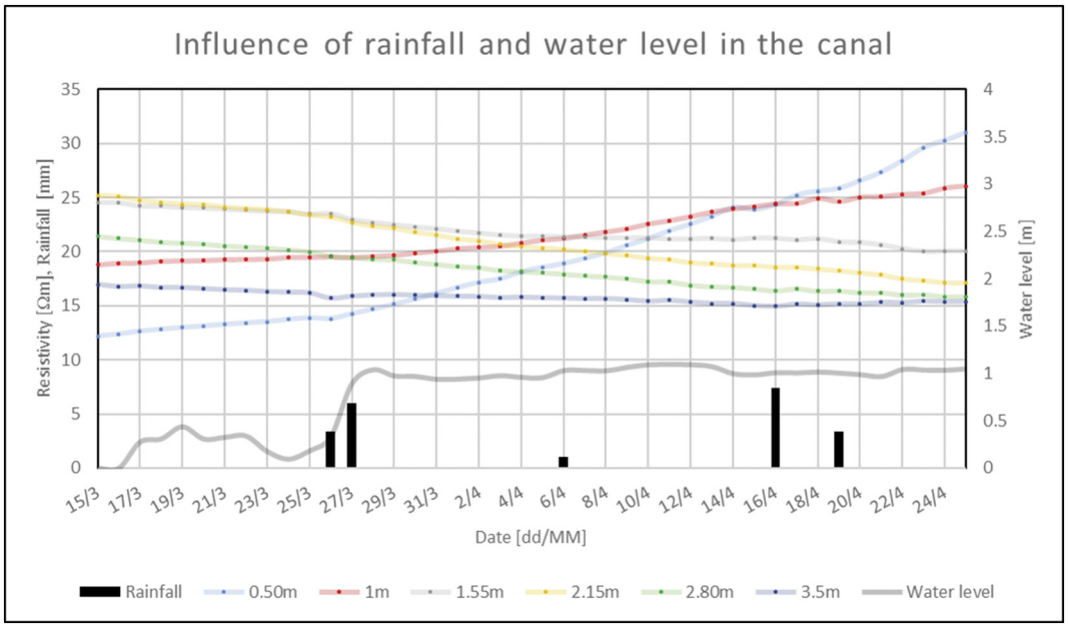

Fig. 13. Influence of rainfall and water level in the canal on resistivity at different depths (15 March – 25 April 2017).

shallow, intermediate and deep parts of the levee (Fig. 14). The top of the embankment is the most sensitive to rainfall events, with resistivity decreasing according to daily cumulative rainfall. Resistivity increases at intermediate depth after rainfalls (see also Fig. 11), while at the bottom of the embankment we find a behavior similar to that of the top part, but with a much slighter decreasing trend.

Fig. 15 shows the relation between the resistivity values averaged at different depths and the water level in the canal for weekly data in 2017 (days close to rainfall events were discarded). Resistivity at shallow depth (0.5 m) increases with the filling of the canal but this is only an apparent reaction. Actually, the water level of the canal is never so high to affect the top 0.5 m of the levee. As a result, the dominating effect in this part of the structure is the drying of the top soil of the levee during the irrigation season, i.e., the summer. On the contrary, the resistivity at intermediate depth decreases with increasing water level because of the seepage through the embankment over time. Finally, the bottom part of the embankment seems to be insensitive to the water level showing an approximately constant resistivity throughout the year.

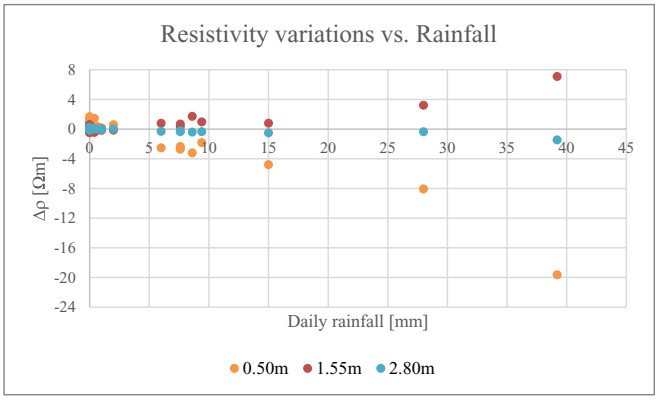

Fig. 14. Scatter plot of resistivity variations at different depths and daily rainfall (15 July – 15 October 2016).

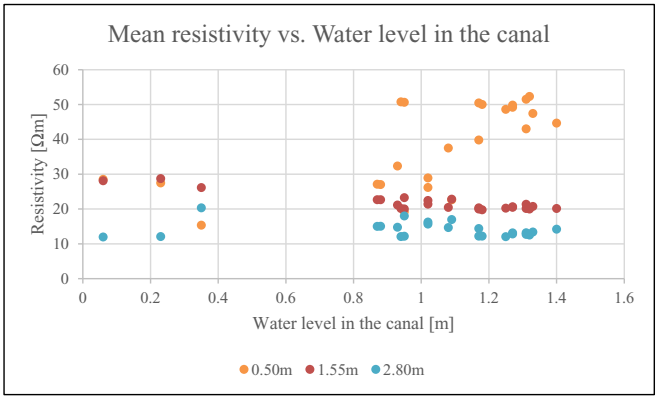

Fig. 15. Scatter plot of the resistivity values averaged at different depths and water level in the canal (2017).

3.2. Relationship between water content and resistivity

In order to estimate water content from resistivity values, we derived an empirical relation by analizing core samples obtained from the levee body. Since resistivity depends on various parameters such as water content, salinity, porosity and lithological structure, a relation between water content and resistivity cannot be found without auxiliary data. Thus, we bored a hole during the irrigation season approximately at the center of the ERT spread down to the depth of 3.30 m and we collected ten samples that were analyzed in the laboratory to determine the water content with the gravimetric method (Table 1).

Analysis of soil grain size was also performed to characterize soil properties of the embankment. Results of sieve and sedimentation analysis are shown in Fig. 16 together with water content values obtained by oven drying. The depth and water content values of the samples are directly proportional while the grain size and the depth are inversely related. All the embankments in the study area are built with local soils, so it is reasonable to assume that the surrounding area has soil with a similar grain size, typical of an alluvial plain. Fig. 16 shows that excluding the shallowest sample, the levee material has a significant percentage of clay. According to this, we tried to estimate a relationship between water content values obtained from the analysis of the samples and inverted resistivity for depths higher than 0.50 m (Fig. 17). It should be mentioned that the resistivity data used for this purpose are the temperature-corrected inverted resistivity data obtained from the ERT measurements on the day of the core sampling. As expected, the calibrated relation between resistivity and water content values in Fig. 17 shows an inverse proportionality. The experimental values were interpolated with a power function and the equation of the fitting curve is shown on the graph.

Table 1
Depths of levee samples and their gravimetric water content values.

Depth (m)	Gravimetric water content (%)
0.48	17.59
0.83	17.69
1.09	19.07
1.2	21.17
1.57	21.89
1.93	20.38
2.26	21.23
2.74	24.80
3.15	28.52
3.3	29.11

For the shallow levee section (< 0.5 m), mainly consisting of sand and with just one sample, we collected new cores from the study site and studied their electrical properties in the laboratory by relating resistivity to TDR measurements. Again, a power function was used to fit the experimental data.

The calibrated relationships were used to convert all the inverted resistivity sections into water content maps. Fig. 18 shows two typical examples of the estimated water content maps for dry and irrigation periods down to a depth of 4 m, corresponding to the height of the levee body. In winter, the saturation of the embankment is more or less homogenous with a water content mainly around 20% (Fig. 18, top). Two more saturated layers are observed at the shallow and bottom parts due to rainfalls. During the summer, saturation increases in the lower half of the levee (depth from 1.5 m to 3 m), because of water flowing in the canal, and saturation decreases in the shallow part as a result of high solar radiation and evapotranspiration (Fig. 18, bottom). No remarkable differences are observed at the base of the levee structure in different periods.

4. Discussion

A prototypal geo-electrical monitoring system was installed on the earthen levee of an irrigation canal and daily data from the resistivity meter and from a meteorological station have been recorded since September 2015. In this work, we analyzed the resistivity variations due to different parameters in the first two years of continuous ERT measurements. In more detail, we studied the influences of temperature, water level in the canal and rainfall on resistivity changes measured at different depths.

We found that daily variations of air temperature affect only the very shallow part of the levee. We analyzed seasonal air temperature trends, whose influence on soil temperature can reach depths higher than 5 m, in order to correct the resistivity datasets and to better understand the effect of other parameters, such as water level in the canal and rainfall.

For our monitored site, water level in the canal is closely related to rainfall, so it is difficult to separate the effects of these two factors. However, our findings suggest that rainfall has a more important role: in the shallow and deep sections of the levee, resistivity values decrease with precipitation, while at intermediate depth we observed an opposite behavior with a fairly rapid increase of resistivity values. Laboratory-scale simulations of the test site are needed to isolate the role of each parameter and to better understand the causes of the observed different resistivity trends.

An issue that is under study is quantifying the 3D effects of the levee geometry on 2D ERT measurements (Arosio et al., 2018; Hojat et al., 2019b). 2D and 3D forward modelings for different water levels in the canal need to be performed to calculate the 3D effects. Our preliminary calculations have shown that 3D effects due to the geometry of the studied levee mainly affect the deeper part of the structure, for the

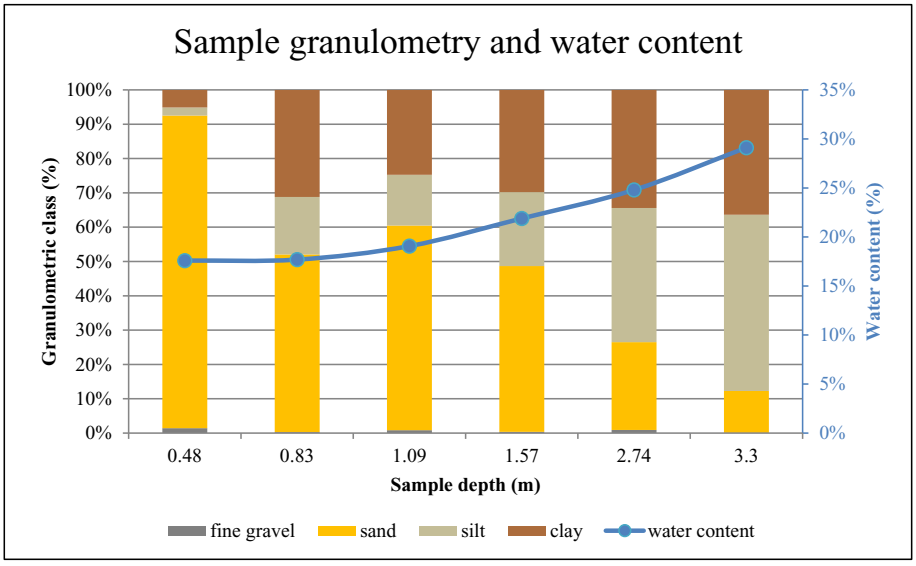

Fig. 16. Grain size and gravimetric water content of levee samples taken at different depths.

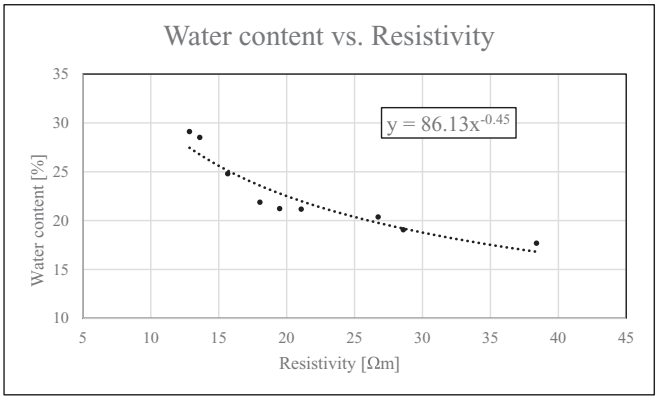

Fig. 17. Gravimetric water content versus resistivity: experimental data (dots) and the fitting curve (dotted line).

effect being more significant in winter. According to simulations, the 3D effects have a maximum of 10% during the irrigation season and a maximum of 25% in the dry period, with the peak of distortion at the base of the embankment. Although 3D effects were neglected so far, they are important on a seasonal time scale. Therefore, comparisons of measurements in short-time periods are nonetheless valid. For example, resistivity variations caused by internal erosion or concentrated seepage on a short period of time can be detected without considering these effects. The next step of our work is to accurately model these effects and to remove their distortion from the data to obtain the unbiased resistivity and water content values.

5. Conclusions

The dependence of resistivity values on changes in the soil water content makes ERT technique a valuable tool to monitor saturation distribution and seepage zones in river levees, giving the opportunity of predicting possible levee breach and of planning proper maintenance

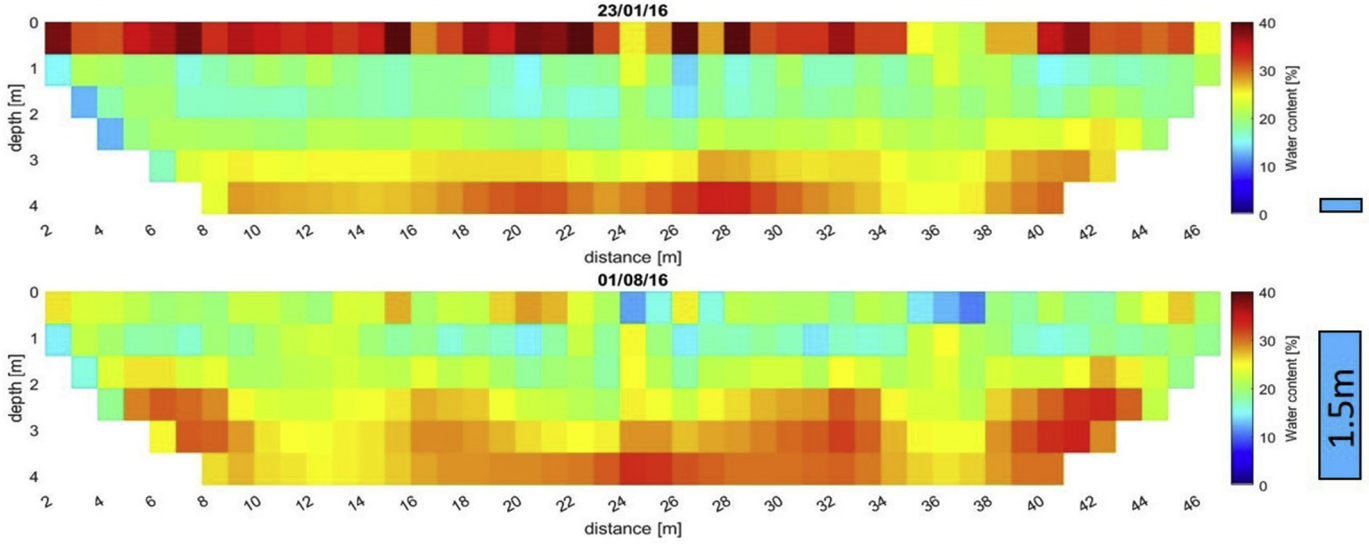

Fig. 18. Examples of water content maps estimated from the inverted resistivity sections in Fig. 4 after temperature corrections. The depth is limited to 4 m, which is the approximate height of the levee structure. Top: 23 January 2016; bottom: 1 August 2016. The light blue bar on the right hand side indicates the water level in the canal at the time of each measurement. (For interpretation of the references to colour in this figure legend, the reader is referred to the web version of this article.)

activities.

The effects of external variables including temperature, water level in the canal and rainfall events on resistivity data were analyzed for different periods of the year and at different depths of the levee structure. Soil temperature variations with the depth were modelled to correct resistivity data for the temperature effect. This effect is of minor importance compared to water level and rainfall effects and thus was studied during periods when other variables are constant or negligible. The influence of variations of the water level in the canal was studied during drawdown processes and at the beginning of the irrigation season. Different electrical behaviors were observed. When the water level is lowered during rainfall events, a sharp variation in resistivity values is recorded, and when the water level is increased, a smooth decreasing trend is recorded. However, since the water level is generally lowered during rainfall events, more studies are required to separate the effect of water level from that of the rainfall.

Rainwater infiltration was also analyzed. When the irrigation canal is full, infiltration can be observed down to a depth of 1.00 m with a decreasing trend in resistivity. On the contrary, increasing resistivity values observed at mid-depth layers could be attributed to the less conductive rainwater replacing the more conductive pore water. In general, shallow and deep parts of the levee experience reduction of resistivity values due to precipitation events and because of the presence of a lateral trench collecting rainwater.

A function to relate water content to resistivity values was calibrated for the levee body below 0.5 m, thanks to core samples taken from the test site. The empirical relationship for the very shallow part where sand content is dominant was obtained from laboratory resistivity and TDR measurements performed on samples coming from the shallow part of the levee. Using these relationships, resistivity sections can be transformed into water content maps that can be used for different purposes, such as stability and seepage analysis.

Acknowledgments

The prototype monitoring system was developed with the technical support of LSI-Lastem Srl. The research work was funded by Fondazione Cariplo, grant no 2016-0785 and by Ministero dell'Ambiente e della Tutela del Territorio e del Mare, project DILEMMA – Imaging, Modeling, Monitoring and Design of Earthen Levees. The authors would like to thank Consorzio di Bonifica Terre dei Gonzaga in Destra Po for the collaboration and assistance in the field. The authors are grateful to the journal editor, Dr. Janusz Wasowski, and the reviewers for their suggestions and thorough reviews that helped to improve the manuscript significantly.

References

Afa, J.T., Anaele, C.M., 2010. Seasonal variation of soil resistivity and soil temperature in Bayelsa State. Am. J. Eng. Appl. Sci. 3 (4), 704–709.

Al-Fares, W., 2014. Application of electrical resistivity tomography technique for characterizing leakage problem in Abu Baara Earth Dam. Syria. Int. J. Geophys. 2014, 368128 (9 pp).

Arosio, D., Munda, S., Tresoldi, G., Papini, M., Longoni, L., Zanzi, L., 2017. A customized resistivity system for monitoring saturation and seepage in earthen levees: installation and validation. Open Geosci. 9, 457–467.

Arosio, D., Hojat, A., Ivanov, V.I., Loke, M.H., Longoni, L., Papini, M., Tresoldi, G., Zanzi, L., 2018. A laboratory experience to assess the 3D effects on 2D ERT monitoring of river levees. In: 24th European Meeting of Environmental and Engineering Geophysics, https://doi.org/10.3997/2214-4609.201802628. Porto.

Asch, T.H., Deszcz-Pan, M., Burton, B.L., Ball, L.B., 2008. Geophysical characterization of American River levees, Sacramento, California, using electromagnetics, capacitively coupled resistivity, and dc resistivity. U.S. Geol. Surv. Open File Rep (2008-1109, 12 pp).

Bakula, K., Salach, A., Wziątek, D.Z., Ostrowski, W., Górski, K., Kurczyński, Z., 2017. Evaluation of the accuracy of lidar data acquired using a UAS for levee monitoring: preliminary results. Int. J. Remote Sens. 38 (8–10), 2921–2937.

Biavati, G., Ghirotti, M., Mazzini, E., Mori, G., Toldini, E., 2008. The use of GPR for the detection of non-homogenities in the Reno River embankments (North-Eastern Italy). In: 4th Canadian Conference on Geohazards: From Causes to Management. Université Laval, Québec, Canada (20–24 May 2008).

Borgatti, L., Forte, E., Mocnik, A., Zambrini, R., Cervia, F., Martinucci, D., Pellegrini, F., Pillon, S., Prizzon, A., Zamariolo, A., 2017. Detection and characterization of animal burrows within river embankments by means of coupled remote sensing and geophysical techniques: Lessons from River Panaro (northern Italy). Eng. Geol. 226, 277–289.

Brunet, P., Clément, R., Bouvier, C., 2010. Monitoring soil water content and deficit using Electrical Resistivity Tomography (ERT) – a case study in the Cevennes area, France. J. Hydrol. 380 (1–2), 146–153.

Busato, L., Boaga, J., Peruzzo, L., Himi, M., Cola, S., Bersan, S., Cassiani, G., 2016. Combined geophysical surveys for the characterization of a reconstructed river embankment. Eng. Geol. 211, 74–84.

Cardarelli, E., Cercato, M., Di Filippo, G., 2010. Geophysical investigation for the rehabilitation of a flood control embankment. Near Surf. Geophys. 8, 287–296.

Cardarelli, E., Cercato, M., De Donno, G., 2014. Characterization of an earth-filled dam through the combined use of electrical resistivity tomography, P-and SH-wave seismic tomography and surface wave data. J. Appl. Geophys. 106, 87–95.

Chambers, J.E., Gunn, D.A., Wilkinson, P.B., Ogilvy, R.D., Ghataora, G.S., Burrow, M.P.N., Tilden Smith, R., 2008. Non-invasive time-lapse imaging of moisture content changes in earth embankments using electrical resistivity tomography (ERT). In: Ellis, Yu, McDowell, Dawson, Thom (Eds.), Advances in Transportation Geotechnics. British Geological Survey, Nottingham, England, pp. 475–480.

Chambers, J.E., Meldrum, P.L., Gunn, D.A., Wilkinson, P.B., Kuras, O., Weller, A.L., Ogilvy, R.D., 2009. Hydrogeophysical Monitoring of Landslide Processes using Automated time-Lapse Electrical Resistivity Tomography (ALERT). Near surface 2009 – 15th European Meeting of Environmental and Engineering Geophysics. (Dublin, Ireland, 7–9 September 2009).

Chambers, J.E., Gunn, D.A., Wilkinson, P.B., Meldrum, P.I., Haslam, E., Holyoake, S., Kirkham, M., Kuras, O., Merritt, A., Wragg, J., 2014. 4D Electrical Resistivity Tomography monitoring of soil moisture dynamics in an operational railway embankment. Near Surf. Geophys. 12, 61–72.

Chlaib, H.K., Mahdi, H., Al-Shukri, H., Su, M.M., Catakli, A., Abd, N., 2014. Using ground penetrating radar in levee assessment to detect small scale animal burrows. J. Appl. Geophys. 103, 121–131.

Cho, I., Yeom, J., 2007. Crossline resistivity tomography for the delineation of anomalous seepage pathways in an embankment dam. Geophys. 72 (2), G31–G38.

Crawford, M.M., Bryson, L.S., 2018. Assessment of active landslides using field electrical measurements. Eng. Geol. 233, 146–159.

Di Prinzio, M., Bittelli, M., Castellarin, A., Rossi Pisa, P., 2010. Application of GPR to the monitoring of river embankments. J. Appl. Geophys. 71, 53–61.

Fauchard, C., Mériaux, P., 2007. Geophysical and Geotechnical Methods for Diagnosing Flood Protection Dikes. Editions Quae, Versailles, France ISBN 978–27592-00313. (128 pp).

Francese, R., Monteiro Santos, F., 2014. Towards a global approach to scan earthen levees. SEG Meeting. (Denver, Colorado, 26-31 October 2014).

Gallipoli, M.R., Lapenna, V., Lorenzo, P., Mucciarelli, M., Perrone, A., Piscitelli, S., Sdao, F., 2000. Comparison of geological and geophysical prospecting techniques in the study of a landslide in southern Italy. Eur. J. Environ. Eng. Geophys. 4, 117–128.

Godio, A., Strobbia, C., De Bacco, G., 2006. Geophysical characterization of a rockslide in alpine region. Eng. Geol. 83, 273–286. https://doi.org/10.1016/j.enggeo.2005.06.034.

Gunn, D.A., Chambers, J.E., Uhlemann, S., Wilkinson, P.B., Meldrum, P.I., Dijkstra, T.A., Haslam, E., Kirkham, M., Wragg, J., Holyoake, S., Hughes, P.N., Hen-Jones, R., Glendinning, S., 2015. Moisture monitoring in clay embankments using electrical resistivity tomography. Constr. Build. Mater. 92, 82–94.

Gunn, D.A., Chambers, J.E., Dashwood, B.E., Lacinska, A., Dijkstra, T., Uhlemann, S., Swift, R., Kirkham, M., Milodowski, A., Wragg, J., Donohue, S., 2018. Deterioration model and condition monitoring of aged railway embankment using non-invasive geophysics. Constr. Build. Mater. 170, 668–678.

Hayley, K., Bentley, L.R., Gharibi, M., Nightingale, M., 2007. Low temperature dependence of electrical resistivity: Implications for near surface geophysical monitoring. Geophys. Res. Lett. 34, L18402.

Hayley, K., Bentley, L.R., Pidlisecky, A., 2010. Compensating for temperature variations in time-lapse electrical resistivity difference imaging. Geophys 75, WA51–WA59.

Hibert, C., Grandjean, G., Bitri, A., Travelletti, J., Malet, J.-P., 2012. Characterizing landslides through geophysical data fusion: example of the La Valette landslide (France). Eng. Geol. 128, 23–29.

Hojat, A., Arosio, D., Longoni, L., Papini, M., Tresoldi, G., Zanzi, L., 2019a. Installation and validation of a customized resistivity system for permanent monitoring of a river embankment. In: EAGE-GSM 2nd Asia Pacific Meeting on near Surface Geoscience & Engineering, https://doi.org/10.3997/2214-4609.201900421. (Kuala Lumpur, Malaysia, 22-26 April 2019).

Hojat, A., Arosio, D., Loke, M.H., Longoni, L., Papini, M., Tresoldi, G., Zanzi, L., 2019b. Assessment of 3D geometry effects on 2D ERT data of a permanent monitoring system along a river embankment. In: EAGE-GSM 2nd Asia Pacific Meeting on near Surface Geoscience & Engineering, https://doi.org/10.3997/2214-4609.201900427. (Kuala Lumpur, Malaysia, 22-26 April 2019).

Inazaki, T., 2007. Integrated geophysical investigation for the vulnerability assessment of earthen levee. SAGEEP 2007. In: Symposium on the Application of Geophysics to Engineering and Environmental Problems, pp. 1–5 Denver, Colorado. (April 2007).

Inazaki, T., Kaneko, M., Aoike, K., 2016. Detailed geophysical imaging of the shallow surfaces at an underseepage site behind of a levee. In: Symposium on the Application of Geophysics to Engineering and Environmental Problems, Austin, Texas, March 22–26 2016.

Jomard, H., Lebourg, T., Guglielmi, Y., Tric, E., 2010. Electrical imaging of sliding geometry and fluids associated with a deep seated landslide (La Clapière, France). Earth Surf. Process. Landf. 35 (5), 588–599. https://doi.org/10.1002/esp.1941.

Karastathis, V.K., KArmis, P.N., Drakatos, G., Stavrakakis, G., 2002. Geophysical methods contributing to the testing of concrete dams. Application at the Marathon Dam. J. Appl. Geophys. 50 (3), 247–260.
Kim, J.-H., Yi, M.J., Song, Y., Seol, S.J., Kim, K.S., 2007. Application of geophysical methods to the safety analysis of an earth dam. J. Environ. Eng. Geophys. 12 (2), 221–235.
Kuras, O., Pritchard, J.D., Meldrum, P.I., Chambers, J.E., Wilkinson, P.B., Ogilvy, R.D., Wealthall, G.P., 2009. Monitoring hydraulic processes with automated time-lapse electrical resistivity tomography (ALERT). Compt. Rendus Geosci. 341 (10), 868–885.
Lapenna, V., Lorenzo, P., Perrone, A., Piscitelli, S., Rizzo, E., Sdao, F., 2005. Case history: 2D electrical resistivity imaging of some complex landslides in Lucanian Apennine (Southern Italy). Geophys. 70, 11–18.
Loperte, A., Soldovieri, F., Palombo, A., Santini, F., Lapenna, V., 2016. An integrated geophysical approach for water infiltration detection and characterization at Monte Cotugno rock-fill dam (southern Italy). Eng. Geol. 211, 162–170.
Morelli, G., Francese, R., 2013. A fast and integrated geophysical imaging system for large scale levee monitoring. In: Symposium on the Application of Geophysics to Engineering and Environmental Problems 2013, (Denver, Colorado, 17–21 March 2013).
Musy, A., Soutter, M., 1991. Physique du sol. Presses polytechniques et universitaires romandes, Lausanne (Collection gérer l'environnement). pp. 348.
Niederleithinger, E., Weller, A., Lewis, R., 2012. Evaluation of geophysical techniques for dike inspection. J. Environ. Eng. Geophys. 17 (4), 185–195.
Panthulu, T.V., Krishnaiah, C., Shirke, J.M., 2001. Detection of seepage paths in earth dams using self-potential and electrical resistivity methods. Eng. Geol. 59, 281–295.
Perri, M.T., Boaga, J., Bersan, S., Cassiani, G., Cola, S., Deiana, R., Simonini, P., Patti, S., 2014. River embankment characterization: the joint use of geophysical and geotechnical techniques. J. Appl. Geophys. 110, 5–22.
Piegari, E., Cataudella, V., Di Maio, R., Milano, L., Nicodemi, M., Soldovieri, M.G., 2008. Electrical resistivity tomography and statistical analysis in landslide modelling: a conceptual approach. J. Appl. Geophys. 68 (2), 151–158.
Samoüelian, A., Cousin, I., Tabbaghc, A., Bruand, A., Richard, G., 2005. Electrical resistivity survey in soil science: a review. Soil Tillage Res. 83, 173–193.
Supper, R., Romer, A., Kreuzer, G., Jochum, B., Ottowitz, D., Ita, A., Kauer, S., 2012. The GEOMON 4D Electrical Monitoring System: Current State and Future Developments. Instrumentation and Data Acquisition Technology. GELMON 2011. (Berichte Geol. B.-A, 93, 23-26, ISSN 1017 – 8880, Vienna, Austria, 30 November-2 December 2011).
Supper, R., Ottowitz, D., Jochum, B., Kim, J.H., Römer, A., Baron, I., Pfeiler, S., Lovisolo, M., Gruber, S., Vecchiotti, F., 2014. Geoelectrical monitoring: an innovative method to supplement landslide surveillance and early warning. Near Surf. Geophys. 12, 133–150.
Takakura, S., Yoshioka, M., Ishizawa, M., Sakai, N., 2013. Measurement of Soil Temperature in the Slope of an Embankment by Using a Large-Scale Rainfall Simulator. (11th SEGJ International Symposium, 248-251, Yokohama, Japan, 18-20 November 2013).
Tresoldi, G., Arosio, D., Hojat, A., Longoni, L., Papini, M., Zanzi, L., 2018. Tech-Levee-Watch: experimenting an integrated geophysical system for stability assessment of levees. Rend. Online Soc. Geol. Ital. 46, 38–43. https://doi.org/10.3301/ROL.2018.49.
Wodajo, L., Hickey, C., 2017. Seismic refraction and electrical resistivity cross-plot analysis of the Francis levee site. In: Symposium on the Application of Geophysics to Engineering and Environmental Problems 2017, (Denver, Colorado, 19–23 March 2017).